UNIVERSITY OF BATH

University of Bath

Alternative formats
If you require this document in an alternative format, please contact:
openaccess@bath.ac.uk

Experimental and Analytical Investigation of the Response of a Triboelectric Generator under Different Operating Conditions

Mohamed A. Elbanna[1], Mustafa H. Arafa[1] and Chris R. Bowen[2]

[1] Mechanical Engineering Department, American University in Cairo, Cairo, Egypt

[2] Mechanical Engineering Department, University of Bath, Bath, BA2 7AY, UK

Abstract

This paper provides experimental and theoretical studies on the effect of operating conditions on the output response of triboelectric generators. The influence of specific parameters is examined in detail, including vibration frequency, impact separation distance and the type of adhesive between the dielectric and the electrode for a single dielectric layer device operating in contact-separation mode, with Teflon and copper being the dielectric and electrode materials, respectively. A scotch-yoke mechanism is designed and fabricated in an effort to understand the effect of varying the operating conditions on the output voltage behavior. The voltage output was compared with an analytical capacitor model at drive frequencies ranging from 1 – 5 Hz and separation distances from 5 – 40 mm in order to evaluate the model's effectiveness in predicting generator output. The experimental results provide new insights into the behavior of triboelectric generators and how the type of adhesive between the dielectric material and the electrode affects the output signal.

Introduction

A substantial amount of research has been expended to develop novel alternatives to traditional energy harvesting and sensing techniques. Triboelectric generators, which produce electric charges when dissimilar dielectric materials are brought into physical contact, have recently been recognized as effective tools for both energy harvesting and sensing. Triboelectrification was introduced by Wang *et. al*. [1] and has been reported to have the potential to not only power nano-scale devices, such as wearable and portable electronics and sensors [2], but can potentially operate at larger scales to harvest energy from human motion and sea waves [3]. It has also been shown to compete with other sources of energy harvesting as it has fewer limiting restrictions, thus it can operate under a variety of conditions; for example a range of dielectric materials can be used [4] as well as any type of contact between plates, friction of contact-separation, and it can produce relatively high voltage at frequencies as low as 1 Hz. Moreover, triboelectric devices can be manufactured from low-cost materials and they are simple to design [5].

The phenomenon of triboelectrification remains a subject of study from the physical point of view [3] [6] and parameters affecting it remain under investigation [7]. The main explanation of the fundamental mechanism is based on the fact that different materials have an affinity to be positively or negatively charged, where the contact of two materials with different affinities can exchange electrons to satisfy this affinity. If a conductive electrode material is added to the back of the contacting material layer, charges can be collected and the two electrodes will act as two terminals of an electrical circuit and on closing the circuit a current will flow.

Several techniques have been explored for triboelectric energy generation, the most used and tested approach is the *contact-separation* mode, where two parallel plates are brought into cyclic contact and separation. Usually, one plate moves while the other is fixed, and each plate is often formed from a dielectric and a conductive electrode attached to its back surface. Other models have been proposed including [5] [4] a *freestanding* mode, where two similar electrodes that are connected through an

electrical load have a dielectric that passes over them, leading to the two electrodes being charged differently and creating a current, or a single electrode mode where the electrode is not attached to the dielectric. In these two cases the dielectric is out of the circuit and interacts with the electrodes either through motion or by touching their surfaces periodically. Some modes are not dependent on contact separation, but rely on friction between the plates, such as the *sliding mode* [5] [4].

In the contact-separation mode, it is not necessary for both plates to be made of a dielectric with an electrode since the device can operate with a single conductive electrode that undergoes a contact-separation action with a dielectric that has an electrode attached to its back surface. In this case both electrodes are used as the electrical terminals of the triboelectric generator, as shown in Figure 1. This is known as a *dielectric-conductor model* and even though it is of lower efficiency than the dielectric-dielectric model, it is considered more applicable where external environment elements can be used to harvest energy, such as air flow or the motion of car tires [6].

Research has explored possible ways to optimize triboelectric generators to achieve an increased power output since its output is known to be of low current and high voltage [6], where several applications may need higher current value to operate. An important aspect is the type of material employed since not all materials have the same level of electron affinity; therefore it is better to use materials with a high positive or negative affinity [3]. Optimization of the device can be achieved through changing the surface roughness of the material on the nano-scale to help achieve an intimate contact between the surfaces [6]. Increasing the surface charge, which is an important factor affecting the produced power, can also be undertaken by ion injection on the surface of the triboelectric surface [8]. Operating the device in a vacuum can also improve the efficiency of the system and produce more power. Placing a flexible layer behind the fixed electrode and allowing it to slightly move during contact can help to increase the intimacy of surface contact and increase power [3]. Optimizing the external circuit has attracted attention [9] where authors have compared the voltages formed on different storage capacitors after charging them with a rectified output of the generator to determine the optimum capacitor. Other work has considered the natural frequency of the system [10] and focused on both the load resistance and the capacitor formed by the triboelectric itself and have derived appropriate figures of merit.

Research effort has also focused on deriving mathematical models which can aid in predicting the behavior of triboelectric generators. The majority of the published work is based on a capacitor model, primarily due to its simplicity, and one of the notable models that deviated from the capacitor model is the approach reported by Dharmasena [11] [12] where the triboelectrification process was explained from an electric field viewpoint. In this case, there is a change in the electric field between the charged surfaces due to a change in the distance between the two plates. This assumption results in a variable potential between the terminals of the two electrodes of the triboelectric generator. Useful theoretical frameworks of triboelectric generators are provided in [13], [14] and [15].

The aim of this paper is to provide an improved understanding of the triboelectric phenomenon by experimentally examining the effect of the important parameters of impact frequency, displacement between the impacting plates and the adhesive type between the electrode and the dielectric on the output voltage. A comparison of the experimental observations with an analytical model will also allow validation of the triboelectric model and help improve its capability of predicting the electrical output behavior.

Theory

Capacitor Model

Power generation during triboelectrification is a result of the electric field generated between the materials. Any material has an affinity to be negatively or positively charged to different levels [10]. This surface charge is based on the Fermi level of the material, relative to vacuum, which is also termed the material *work function*. Materials with a high work function tend to gain electrons, and hence become negatively charged upon contact, while materials with a low work function tend to lose electrons. Upon sliding two materials of different affinity against each other, or impacting them against each other during contact-separation, there will be an intimate contact and electron exchange between the surfaces. One plate will experience positive charge accumulation on the surface while the other will experience a negative charge accumulation on its surface, hence an electric field will be generated between them. This will cause the electrode attached to each plate to be charged by an opposite charge and connecting the two electrodes through a circuit will result in a current flow through the circuit due to the potential difference. When using a dielectric and electrode combination against a single electrode, the single electrode will do the work of both the impacting plate and the electrode, as shown in Figure 1. As a result, charges will be on both of its surfaces. A number of researchers have attempted to develop a mathematical model for this phenomenon and one of the most used analogies is the capacitor model [1,4,7-9]. This model assumes that the two charged opposing electrodes can be considered as two capacitor plates with two dielectrics between them; a dielectric of fixed thickness which represents the material used to create the electrode and a dielectric of varying thickness which represents the air between the plates. In this work, Teflon was chosen as the dielectric material as it is located at the bottom of the triboelectric series and therefore has a high negative affinity [4]. The dielectric then is considered to be of a variable capacitance and equations have been developed using capacitive equations in an effort to predict the generated electrical energy behavior of the triboelectric generator [13].
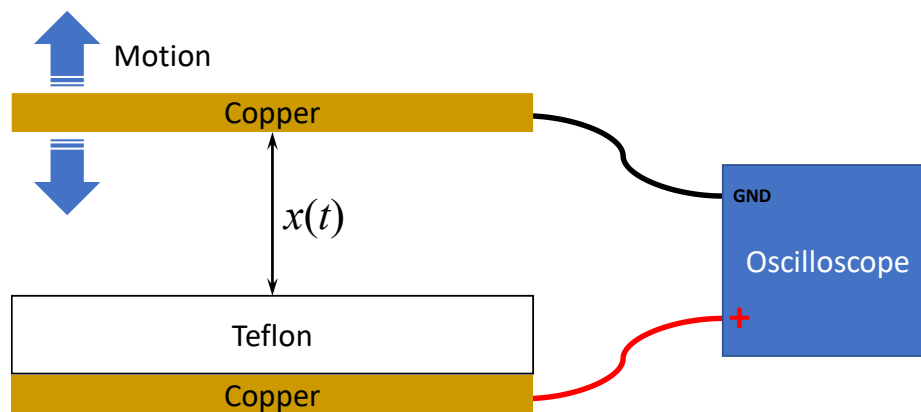

Figure 1 Schematic of the model used, with a single upper metallic electrode and lower electrode attached to a dielectric.

Capacitor Model Equations

We now describe the capacitor model [13], where the capacitance between the plates is defined as,

$$C = \varepsilon_0 \frac{A}{d} \tag{1}$$

Where *C* is the capacitance in Farads, ε_0 is the air/vacuum permittivity, where ε_0 = 8.85x10^{-12} F/m , *A* is the surface area of the capacitor plates and *d* is the distance between the plates.

The voltage is given by,

$$V = \frac{Q}{C}$$ (2)

Where *V* is the voltage from the capacitor and *Q* is the charge on the capacitor plates in Coulombs. By varying *d* in equation (1), the value of *C* changes which results in a change in the voltage across the capacitor (for a given charge) to change and affect any component with the capacitor in the circuit.

This approach assumes that charges accumulate on the surface of the dielectric and are equally distributed with a uniform surface charge density, σ, which is later defined as the triboelectric charge density on the electrodes. This includes the electrode that comes in contact and separation with the dielectric and the electrode attached to the dielectric that accumulates charges on their surface with charge densities of σ_1 and σ_2 respectively. The capacitor, formed from the triboelectric generator, together with the load resistance, forms a closed circuit with the following conditions satisfied:

$$\sigma_1 + \sigma_2 - \sigma = 0$$ (3)

$$\sum V = 0$$ (4)

Equation (3) is a result of the conservation of charges and equation (4) is due to Kirchoff's law of a closed circuit.

The capacitor formed by this triboelectric generator has two dielectric mediums; air and the dielectric material (Teflon in this work), producing two electric fields inside.

$$E_a = \frac{-\sigma_1}{\varepsilon_0}$$ (5)

$$E_d = \frac{-\sigma_2}{\varepsilon_0 \varepsilon_r}$$ (6)

Equation(5) describes the electric field formed in the air gap between the charged surface on the free electrode and the charged surface on the dielectric plate while Equation (6) describes the electric field formed in the dielectric material itself between its charged surface and the dielectric connected to it as seen in Figure 2. ε_r is the relative permittivity, which is dimensionless and a property of the dielectric material, namely Teflon.
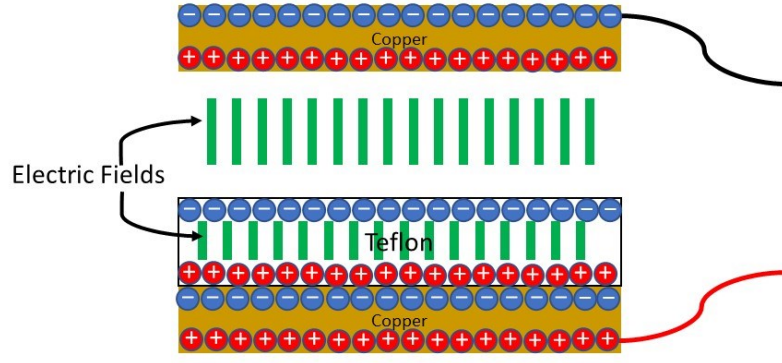
Figure 2 Schematic for the charge arrangement and electric fields in the triboelectric generator during operation

Converting these electric fields into voltages and substituting into equation (4) for the circuit and assuming that the voltage across the load resistance is *V(t)*, the result is equation (7)

$$E_a x(t) + E_d d + V(t) = 0 \tag{7}$$

where $x(t)$ is the varying gap/air distance between the plates, termed the separation distance. Assuming that Q represents the charge that moves between the electrodes and through the load resistance, which is zero at the start of operation (equation (8)), then

$$Q_{t=0} = 0 \tag{8}$$

The conversion of these charges to charge density on the surface of the electrodes (equation (9)), where S is the area of the plates, is given by

$$\sigma_2 = \frac{Q}{S} \tag{9}$$

Substituting equations (3) and 9 in equations (5) and equations (9) in equation (6), the following equations are derived:

$$E_a = \frac{\sigma_2 - \sigma}{\varepsilon_0} = \frac{Q}{S\varepsilon_0} - \frac{\sigma}{\varepsilon_0} \tag{10}$$

$$E_d = \frac{Q}{S\varepsilon_0 \varepsilon_r} \tag{11}$$

In order to convert the charge to the voltage across the load resistance it must be differentiated with time and multiplied by the value of the load resistance:

$$V(t) = R \times I(t) = R \times \frac{dQ}{dt} \tag{12}$$

Substituting equations (10),(11) and (12) in equation (7) yields:

$$\left[\frac{Q}{S\varepsilon_0} - \frac{\sigma}{\varepsilon_0}\right] x(t) + \frac{Q}{S\varepsilon_0 \varepsilon_r} d + R \times \frac{dQ}{dt} = 0 \tag{13}$$

Defining d_0 as effective thickness constant and substituting back in equation (13)

$$d_0 = \frac{d}{\varepsilon_r} \tag{14}$$

$$\frac{Q}{S\varepsilon_0}x(t) + \frac{Q}{S\varepsilon_0}d_0 - \frac{\sigma}{\varepsilon_0}x(t) + R \times \frac{dQ}{dt} = 0 \qquad (15)$$

$$R \times \frac{dQ}{dt} + \frac{Q}{S\varepsilon_0}(x(t) + d_0) - \frac{\sigma}{\varepsilon_0}x(t) = 0 \qquad (16)$$

Equation (16) can then be solved in order to find the charge moving in the circuit Q as a function of time, from a differential equation the following equation is derived:

$$Q(t) = \left[\int_0^t \frac{\sigma x(\tau)}{R\varepsilon_0} e^{\int_0^\tau \frac{d_0 + x(z)}{RS\varepsilon_0}dz} d\tau \right] e^{-\int_0^t \frac{d_0 + x(\tau)}{RS\varepsilon_0}d\tau} \qquad (17)$$

Differentiating equation (17) will result in the circuit current produced form the triboelectric generation. Multiplying this current with the load resistance will result in a voltage across it.

$$I(T) = \frac{dQ}{dt} = \frac{\sigma x(t)}{R\varepsilon_0} - \frac{d_0 + x(t)}{RS\varepsilon_0} e^{-\int_0^t \frac{d_0 + x(\tau)}{RS\varepsilon_0}d\tau} \int_0^t \frac{\sigma x(\tau)}{R\varepsilon_0} e^{\int_0^\tau \frac{d_0 + x(z)}{RS\varepsilon_0}dz} d\tau \qquad (18)$$

$$V(t) = R \times I(T) = \frac{\sigma x(t)}{\varepsilon_0} - \frac{d_0 + x(t)}{S\varepsilon_0} e^{-\int_0^t \frac{d_0 + x(\tau)}{RS\varepsilon_0}d\tau} \int_0^t \frac{\sigma x(\tau)}{R\varepsilon_0} e^{\int_0^\tau \frac{d_0 + x(z)}{RS\varepsilon_0}dz} d\tau \qquad (19)$$

Equations (18) and (19) are solved numerically to provide the theoretical predictions of the proposed capacitor model where R is the resistance of the oscilloscope used to measure the output voltage.

Experimental Methods

A motor-driven Scotch-yoke mechanism was designed (Figure 3) and fabricated (Figure 4) to test the contact-separation triboelectric generator under controlled drive conditions. This mechanism is known to provide a purely sinusoidal displacement which is considered a good reference signal for dynamic testing. The frequency of impact can be adjusted by the stepper motor speed and the stroke (separation distance) can be varied by changing the crank length. As illustrated in Figure 3, the device moves a copper electrode cyclically to impact a fixed multi-layer target consisting of a Teflon sheet with a copper electrode backed by a foam layer onto a rigid support whose position can be adjusted to accommodate for different strokes or to allow the foam layer squeeze during operation, if desired. Experiments were conducted to determine the relationship between the electrical voltage produced and the frequency of impact, the type of the Teflon-electrode adhesive and the maximum separation distance between the two plates of the triboelectric generator. The Teflon used has a measured relative permittivity of ε_r= 3.6 and measured 180 mm in length, 95 mm in width and 0.3 mm in thickness with copper tape attached to its back surface to act as an electrode, see Figure 1. The Teflon films with the copper tape were fixed using four screws to the fixed plate with a foam layer between them to allow the plates to 'squeeze' during operation if needed. This triboelectric generator was operated at five separation distances, namely 5, 10, 20, 30, and 40 mm, at five impact frequencies, namely 1, 2, 3, 4 and 5 Hz. The voltage generated was measured using an oscilloscope, with an internal resistance of 10 MΩ, where the positive peak value, the negative peak value and the peak-to-peak value of the produced voltage was recorded. The electrode attached to the Teflon was connected to

the positive terminal of the oscilloscope probe while the single electrode was attached to the negative probe.
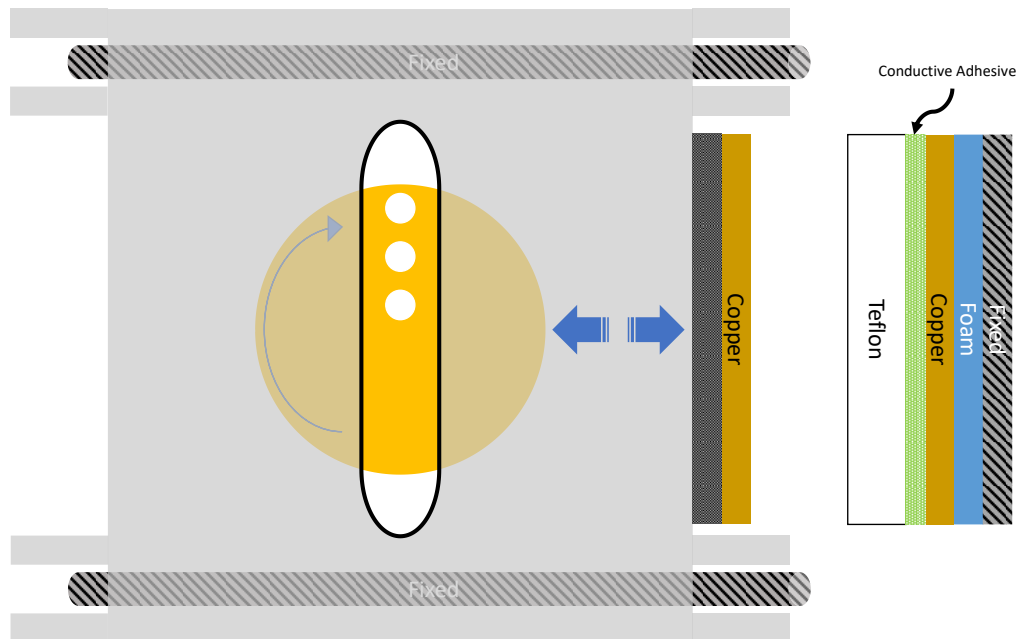

Figure 3 Sketch of the mechanism (top view) where the scotch yoke mechanism forces the grey platform to move in a straight line guided by the fixed rods allowing the Teflon and the copper to be in constant contact and separation with a variable displacement due to the variable pin positions connecting the scotch and the yoke.
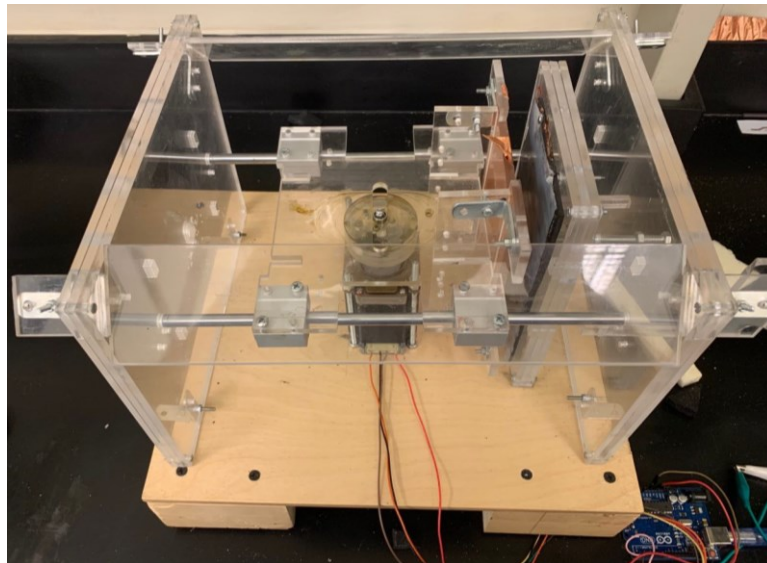

Figure 4 Device used in experimentation, the electrodes can be seen on the right hand side of the image. Linear bearings are used as guides to reduce sliding friction.

In order to test the effect of the conductive adhesive type between the dielectric (Teflon) and the electrode (copper) on the electrical energy output of the generator, the experiment was repeated twice. For the first trial, a conductive adhesive copper tape was used and the adhesive side was bonded directly to the Teflon. In the second trial a conductive carbon-based epoxy (hardener and resin mix) was used to adhere the non-sticky copper side to the Teflon, i.e. the plain copper side without using the adhesive to the Teflon.

Preliminary testing demonstrated that upon starting the experiment the output of the triboelectric generator increases with time until a saturation point is reached and consistent peaks are subsequently obtained. This is due to the saturation of the Teflon surface with charges [13]. It was shown through experimentation that a rapid way to saturate the Teflon surface before running the experiment was to rub the Teflon surface with a copper layer where the friction between them will cause the Teflon surface to become saturated with charge. Therefore, at the start of each experiment, the device was operated at frequency of 5 Hz of contact separation motion and then it was stopped to rub the Teflon surface in the generator with a copper layer and then operated again to compare the output voltage before and after each rub. This was repeated until consistent voltage peaks were achieved, after which the device was operated for 10 minutes at 5 Hz to ensure repeatability, then data was recorded. Before running each displacement, it was made sure that the distance between the plates was exactly the stroke of the device to avoid any 'over squeezing', which can influence the produced results. The different operating conditions employed in this work are shown in Table 1.

Table 1 Operating conditions for triboelectric experimental.

Operating condition	Range or description
Drive frequency	1, 2, 3, 4, 5 Hz
Separation distance	5, 10, 20, 30, 40 mm
Type of adhesive between dielectric and electrode	Conductive adhesive copper tape or copper tape with epoxy adhesive

Results and Discussion

Sample time-domain voltage signals are shown in Figure 5(a) and Figure 5(b) for different strokes and frequencies.
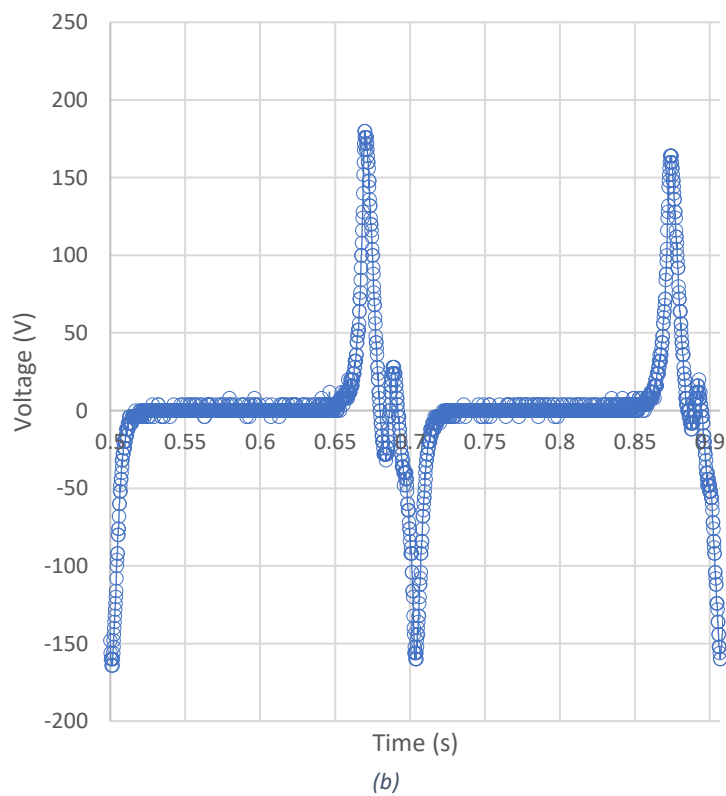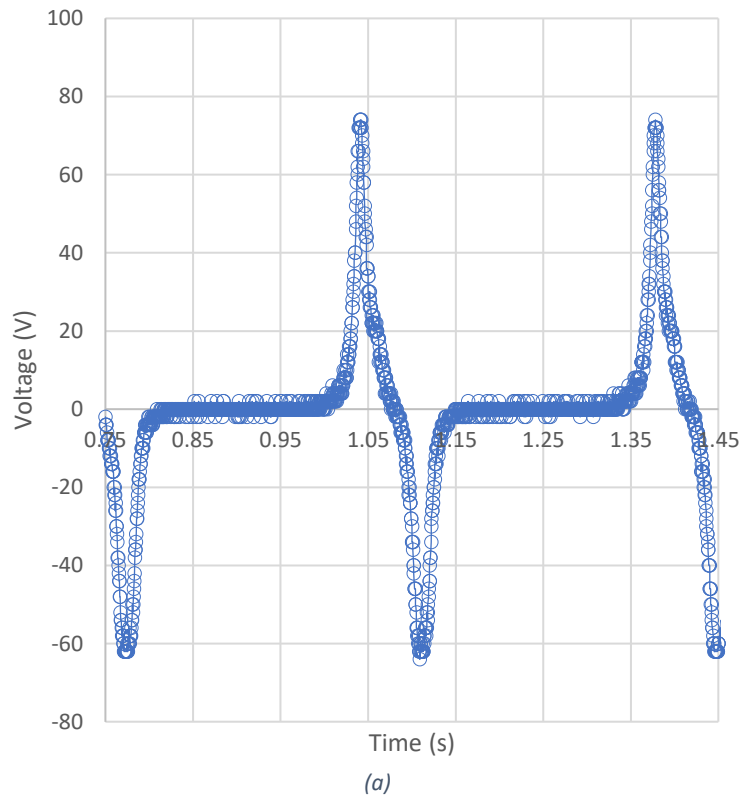

(a)

(b)

Figure 5: (a) Teflon with conductive adhesive copper tape as electrode at stroke 20 mm and frequency 3 Hz
(b) Teflon with conductive adhesive copper tape as electrode at stroke 40 mm and frequency 5Hz

Figure 5(a) shows an ideal form of wave where it peaks to a positive value then falls to a negative value (smaller in magnitude), in agreement with the waveform reported in [13]. However, Figure 5(b) shows an example of another output from the device, where there is a falling notch after the positive peak that increases again before decreasing to the negative peak. This can be a result of the differences in surface flatness of the Teflon which can result in some 'squeezing' of the surfaces together. The positive peak corresponds to the moment of impact, while the negative peak occurs during separation. It was assumed that after saturation the charges on the surface remained constant during the operation.

The positive peak was the main consideration in our analysis since it was often of better quality than the negative peak, especially at high speeds. This can be due to the fact that the positive peak is produced from the impact (the electrode is moving towards the Teflon sheet) while the negative peak is produced by the release (the electrode is moving away from the Teflon sheet) and since the plates may have squeezed together, it could have affected the separation motion than the impact. It can also be noted that at higher speed the positive peak turned into a sharper peak while in case of slow speeds the peak was rather flat which can be related to the squeezing i.e. the plates impacted and remained in contact for a while before they started separating. The results are summarized in Figure 6 and Figure 7, which show the positive peak voltage taken at steady-state conditions.
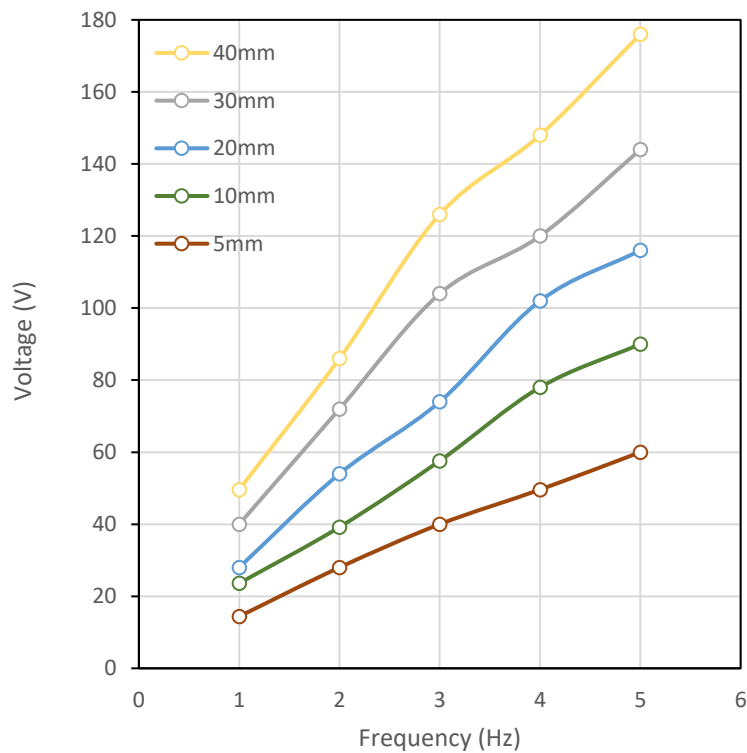

(a)
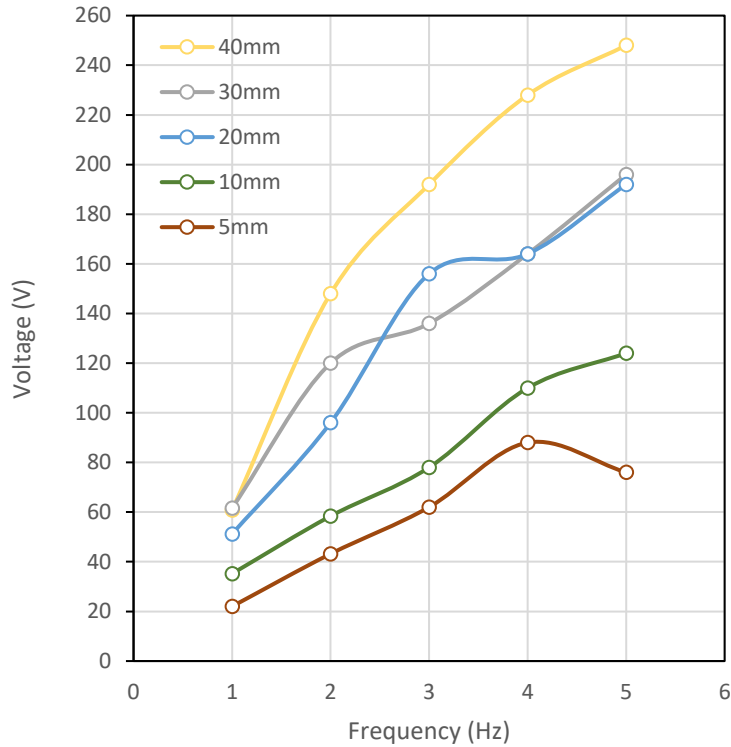
(b)

Figure 6: Positive peak voltage versus frequency at different displacements using (a) copper adhesive tape as electrode, and (b) epoxy and copper as electrode

It is clear from Figure 6(a) and Figure 6(b) that the separation distance and the frequency of the impact affects the output voltage of the generator, where an increase in frequency or separation increases the voltage. In addition, at high separation distances the influence of the frequency increases, due to the higher slope, where an increase in frequency from 1 Hz to 5 Hz for the adhesive copper tape electrode, Figure 6(a), increased the voltage from 49.6 V to 176 V at an impact amplitude of 40 mm compared to a smaller increase from 14.4 V to 60 V at a lower separation of 5 mm. The same behavior can be observed in case of the epoxy bonded generator, Figure 6(b).

Since Teflon is a 'non stick' material that prevents regular adhesives from sticking to its surface, it produced different results when two different types of adhesives were used between the Teflon and the copper electrode. The conductive carbon based epoxy (hardener and resin) was found to provide a better output in the form of higher voltage values as compared to using the conductive adhesive in the copper tape.
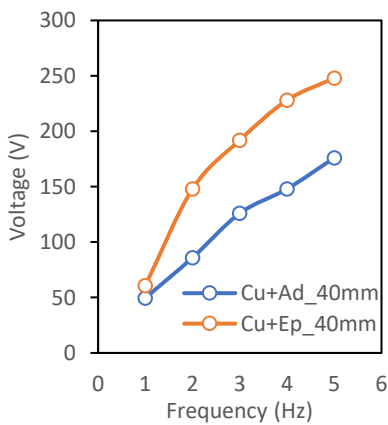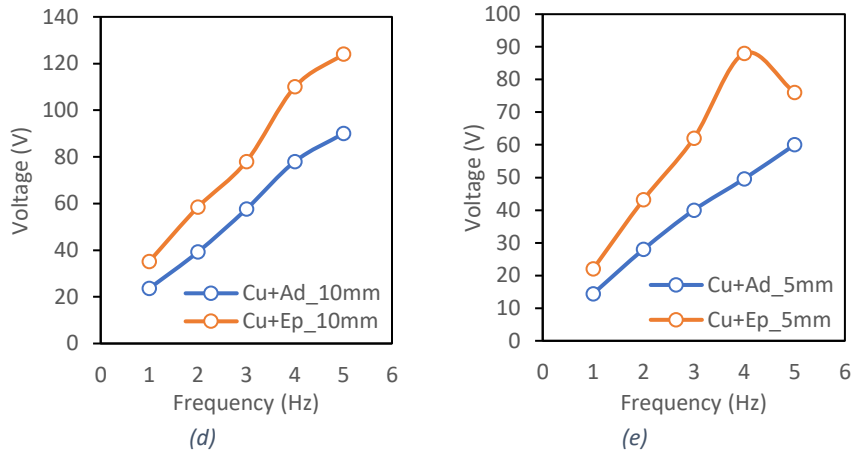

(a)
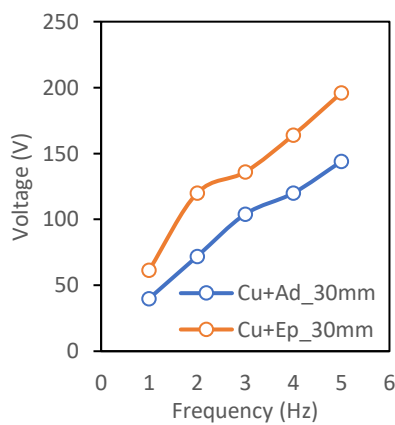
(b)
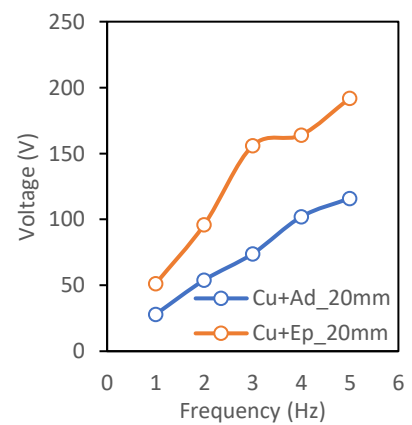
(c)

Figure 7: Positive peak voltage obtained when using adhesive copper tape and copper with epoxy for a displacement of (a) 40 mm; (b) 30 mm; (c) 20 mm; (d) 10 mm; (e) 5 mm.

It can be observed in Figure 7 that the type of the adhesive between the copper layer used as electrode and the dielectric (Teflon) influences the voltage output, where using the epoxy between the Teflon sheet and the copper increased the output voltage compared to the conductive adhesive of the copper tape. While the negative peaks are not as clear as the positive peaks, similar trend lines were observed; see Figure 8.
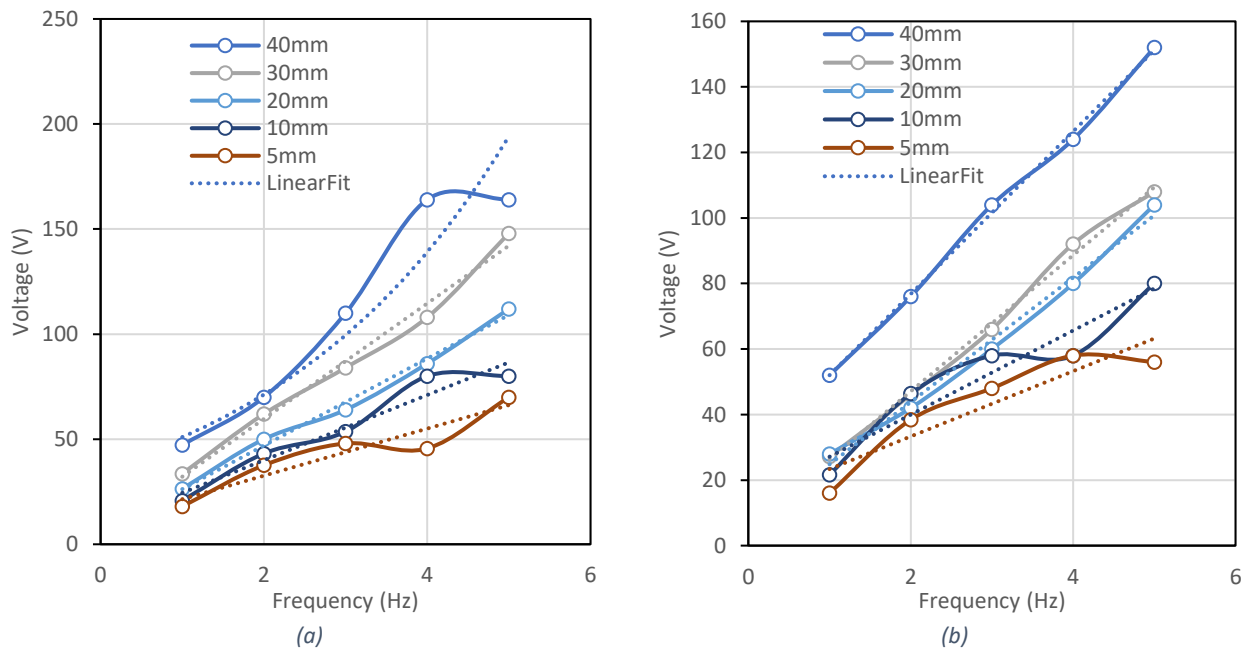

Figure 8 Negative peak voltage versus frequency at different displacements using (a) adhesive copper tape as electrode; (b) copper with epoxy as electrode

An additional experiment was conducted with Teflon and a copper tape electrode where it was squeezed with the moving electrode using a foam padding shown in Figure 3 to aid in producing a higher voltage due to an enhanced contact, as in Figure 9. In this case the voltage is clearly much higher than the non-squeezed experiment in Figure 5(b). It is noted that the applied excitation in this work is displacement-controlled, as provided by the scotch-yoke mechanism. While the force was not measured experimentally, its effect clearly indicates that higher forces lead to a better contact, which results in a higher voltage output, as shown in Figure 9.
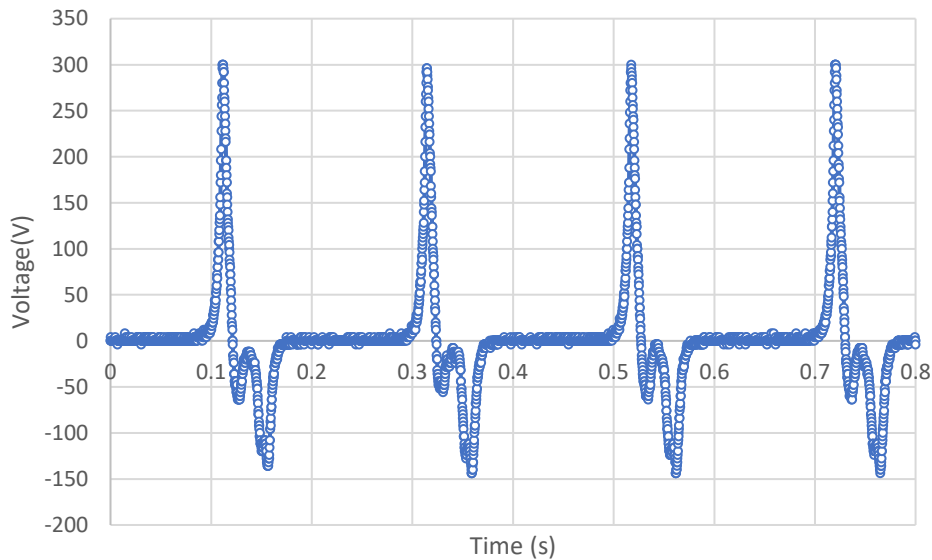

Figure 9 Squeezed Teflon with copper tape as electrode with stroke 40 mm at 5Hz

For the analytical model, due to the difficulty of measuring the surface charge density, which is needed to calculate the triboelectric voltage, the surface charge density was obtained twice from the experimental data and by fitting to the data of the Teflon with the copper adhesive tape as an electrode at a stroke of 40mm and a frequency of 5Hz for the first instance and at a stroke of 20mm and a frequency of 3Hz for a second instance. The equations were solved for different values of surface charge density, until the voltage predicted by the model was in agreement with that obtained experimentally. In this case the charge density obtained was of a value 18.35 $\mu C/m^2$ in case of 40mm stroke and 5Hz frequency, and this is similar to some of the values in the literature such as Yang *et al.* [13] who obtained 15 $\mu C/m^2$, while using a different material. On the other hand, the charge density obtained in case of 20mm stroke and 3Hz frequency was 9.909 $\mu C/m^2$. It has also been reported that the charge density, which is induced by the mechanical loading and affected by the contact force, can range between 5-40 $\mu C/m^2$. These values can be increased using ion injection and can be limited to the air break down voltage so it can be operated in vacuum to achieve higher charge densities [3]. The derived value of 9.909 $\mu C/m^2$ was used to obtain the prediction results shown in Figure 10.
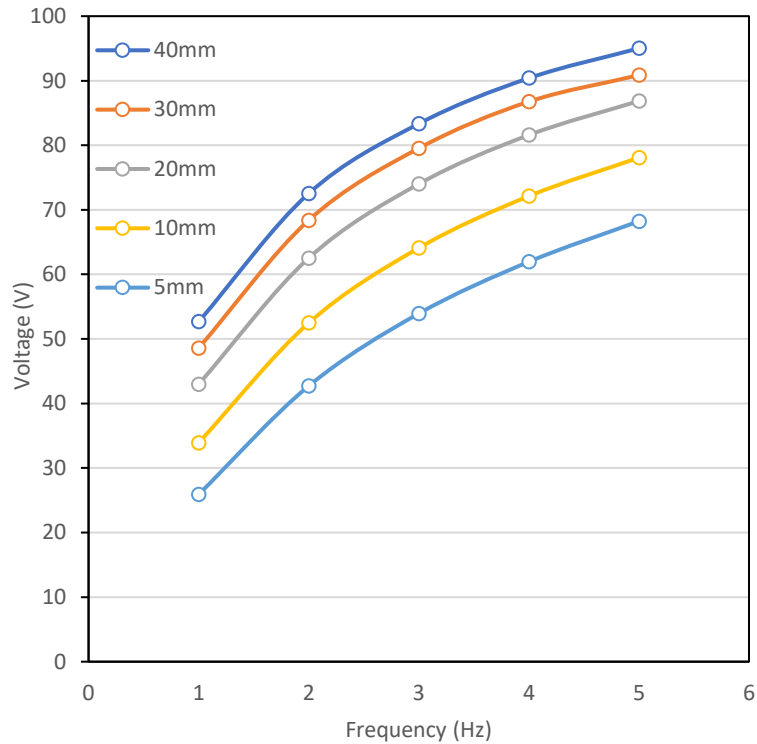
Figure 10 Predicted positive peak voltage of the analytical results for different frequencies and separation at a charge density 9.909 $\mu C/m^2$

The analytical results shown in **Figure 10** appear to agree well with the experimental results of **Figure 6**. Both indicate an increase in voltage with impact distance and frequency, despite the more progressive or divergent experimental voltage-frequency curves (**Figure 6**) as compared to the analytical predictions (**Figure 10**), which look more parallel. The experimental results indicate the voltage will continue to increase with increasing separation distance and frequency, whereas the simulated results suggest some saturation will take place. Figure 11 shows an example of the simulated output voltage based on the equation (19). The first peak is higher than the following peaks, in agreement with [13], and this was not observed in the experimental data because only steady-state measurements were taken.
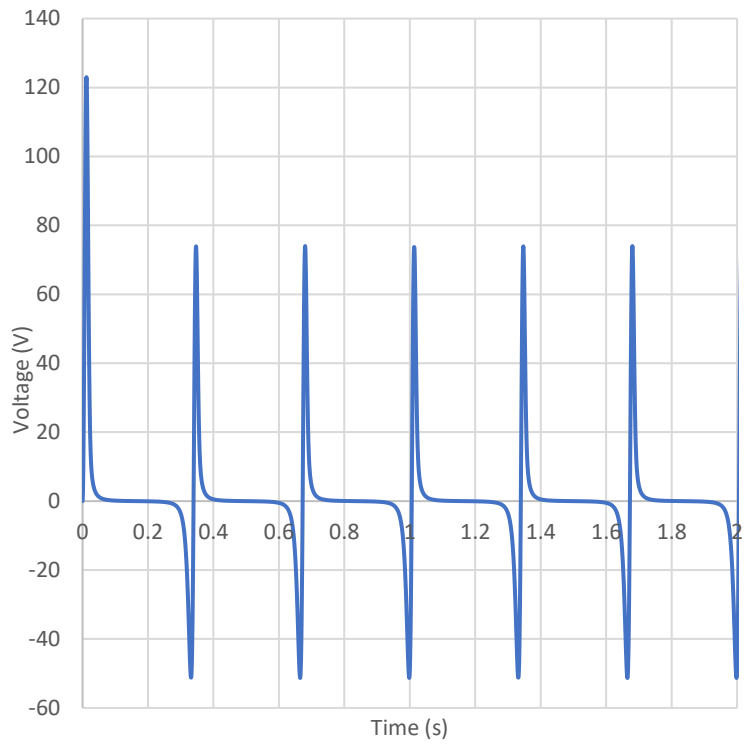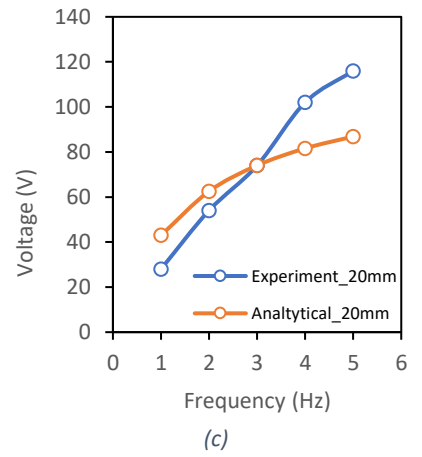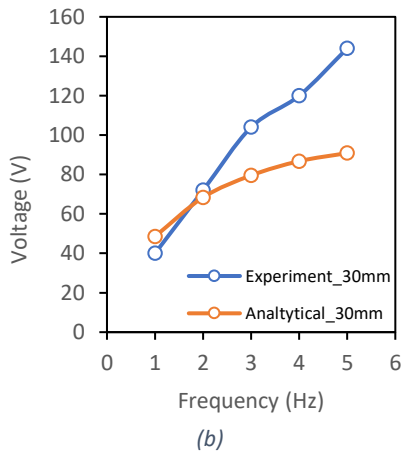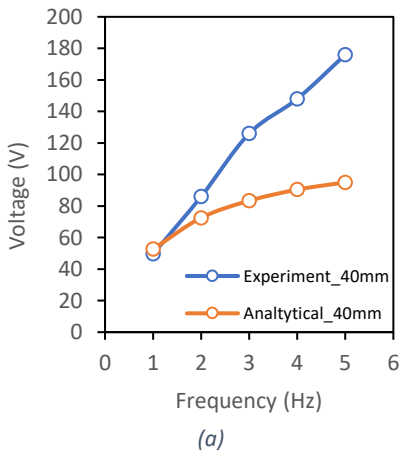
Figure 11 Analytical results at a stroke of 20mm, speed of 3Hz and a charge density of 9.909 $\mu C/m^2$

(a)

(b)

(c)

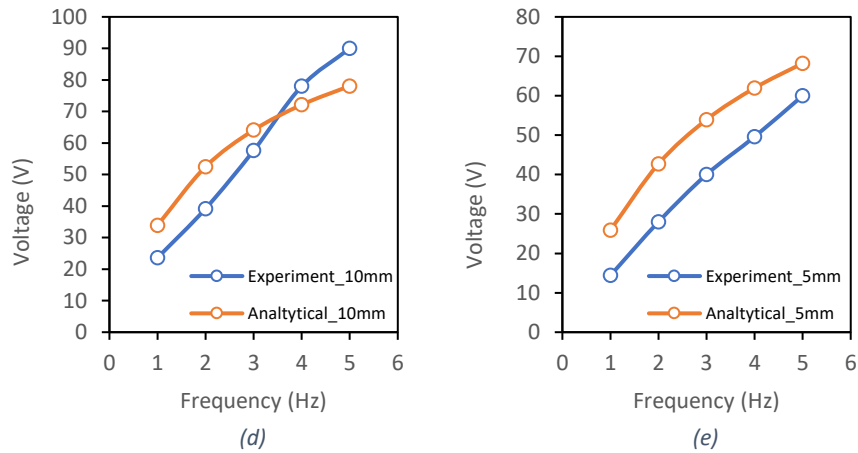*Figure 12 Positive peak of experimental voltage vs analytical solution assuming a charge density of 9.909 μC/m² for a displacement of (a) 40 mm; (b) 30 mm; (c) 20 mm; (d) 10 mm; (e) 5 mm.*

The general trends depicted by the analytical predictions in Figure 12 indicate an increase in voltage with frequency for all separation distances, which agrees with the experimental observations. However, differences in slopes of both curves cause them to intersect, except for the case of a separation distance of 5mm, where the curves seem offset but somewhat parallel. Differences between the analytical and the experimental results shown can be attributed to the inherent approximations in the model. For example, the triboelectric generator has two dielectric materials (air and Teflon) and the air thickness is changing, which affects the output signal. Furthermore, the bonding material is not included in the analytical equations and the electrodes do not fully cover the dielectric surface in the real device, which was illustrated by the two different electrode adhesive types used. Inefficient or non-uniform electrodes affect electron exchange between the Teflon and copper, which leads to errors in the charge density. Finally, the assumed surface charge density can change during the running of the experiment due to leakage and the assumption that all surfaces have the same charge with different signs has some limitations. Parasitic effects can also lead to a loss of produced power [16], such as parasitic capacitance [10]. All these factors contribute to discrepancies between the experimental and the analytical results. As a test the triboelectric generator's performance, it was successful in illuminating light emitting diodes (LEDs) in series with no resistor.

Conclusion

There is a significant potential for using triboelectric generators as energy harvesters from several sources in the environment, and effort is focused to maximize the power produced. This paper is aimed at the study of several design aspects and operating conditions, namely the speed of impact (i.e. vibration frequency), the impact separation distance and type of adhesive between the dielectric and electrode on the voltage generated by triboelectric devices. An increase in both the speed of impact and separation distance between the electrodes leads to an increase in the produced output voltage. This is in good agreement with analytical predictions based on the capacitor model which is widely used to analyze triboelectric generators. Short circuit current was not measured in the present work, and open circuit voltage was used instead as an indicator due to its ease of measurement. More accurate assessment of the output power can be obtained by charging a capacitor or by measuring the short circuit current. The experimental trends seem to have different slopes and relations with one another in comparison with the analytical curves. This can be attributed to various limitations in the analytical model, one of which is the adhesive between the dielectric and the electrode, whose nature influences the generated voltage. The adhesive layer itself can be considered an intermediate electrode if its thickness surpasses a certain threshold. This opens the door for further studies to produce a better adhering substance between the dielectric and the electrode and to develop further

models to account for factors such as surface roughness. This provides insights into future development of triboelectric generators at an experimental, operational, modelling and manufacturing level. Materials and devices engineering plays a pivotal role in such a development.

References

[1] F. R. Fan, Z. Q. Tian and Z. Lin Wang, "Flexible triboelectric generator," *Nano Energy,* vol. 1, no. 2, pp. 328-334, 3 2012.

[2] S. S. Kwak, H. J. Yoon and S. W. Kim, *Textile-Based Triboelectric Nanogenerators for Self-Powered Wearable Electronics,* vol. 29, Wiley-VCH Verlag, 2019.

[3] J. Wang, C. Wu, Y. Dai, Z. Zhao, A. Wang, T. Zhang and Z. L. Wang, "Achieving ultrahigh triboelectric charge density for efficient energy harvesting," *Nature Communications,* vol. 8, no. 1, 1 12 2017.

[4] Z. L. Wang, L. Lin, J. Chen, S. Niu and Y. Zi, Green Energy and Technology Triboelectric Nanogenerators, Springer, 2016.

[5] H. Zhang, L. Quan, J. Chen, C. Xu, C. Zhang, S. Dong, C. Lü and J. Luo, "A general optimization approach for contact-separation triboelectric nanogenerator," *Nano Energy,* vol. 56, pp. 700-707, 1 2 2019.

[6] Y. Wang, Y. Yang and Z. L. Wang, "Triboelectric nanogenerators as flexible power sources," *npj Flexible Electronics,* vol. 1, no. 1, 27 9 2017.

[7] R. D. G. Dharmasena, J. H. Deane and S. R. P. Silva, "Nature of Power Generation and Output Optimization Criteria for Triboelectric Nanogenerators," *Advanced Energy Materials,* vol. 8, no. 31, 5 11 2018.

[8] S. Wang, Y. Xie, S. Niu, L. Lin, C. Liu, Y. S. Zhou and Z. L. Wang, "Maximum Surface Charge Density for Triboelectric Nanogenerators Achieved by Ionized-Air Injection: Methodology and Theoretical Understanding," *Advanced Materials,* vol. 26, no. 39, pp. 6720-6728, 21 8 2014.

[9] Khushboo and P. Azad, "Triboelectric nanogenerator based on vertical contact separation mode for energy harvesting," in *Proceeding - IEEE International Conference on Computing, Communication and Automation, ICCCA 2017*, 2017.

[10] J. Peng, S. D. Kang and G. J. Snyder, "Optimization principles and the figure of merit for triboelectric generators," *Science Advances,* vol. 3, no. 12, 1 12 2017.

[11] R. D. Dharmasena, K. D. Jayawardena, C. A. Mills, J. H. Deane, J. V. Anguita, R. A. Dorey and S. R. Silva, "Triboelectric nanogenerators: Providing a fundamental framework," *Energy and Environmental Science,* vol. 10, no. 8, pp. 1801-1811, 1 8 2017.

[12] R. D. Dharmasena, K. D. Jayawardena, C. A. Mills, R. A. Dorey and S. R. Silva, "A unified theoretical model for Triboelectric Nanogenerators," *Nano Energy,* vol. 48, pp. 391-400, 1 6 2018.

[13] B. Yang, W. Zeng, Z. H. Peng, S. R. Liu, K. Chen and X. M. Tao, "A Fully Verified Theoretical Analysis of Contact-Mode Triboelectric Nanogenerators as a Wearable Power Source," *Advanced Energy Materials,* vol. 6, no. 16, 24 8 2016.

[14] S. Niu and Z. L. Wang, "Theoretical systems of triboelectric nanogenerators," *Nano Energy,* vol. 14, pp. 161-192, 25 10 2014.

[15] S. Niu, S. Wang, L. Lin, Y. Liu, Y. S. Zhou, Y. Hu and Z. L. Wang, "Theoretical study of contact-mode triboelectric nanogenerators as an effective power source," *Energy and Environmental Science,* vol. 6, no. 12, pp. 3576-3583, 12 2013.

[16] J. Chen and Z. L. Wang, *Reviving Vibration Energy Harvesting and Self-Powered Sensing by a Triboelectric Nanogenerator,* vol. 1, Cell Press, 2017, pp. 480-521.